

A Neural Network Architecture for Automatic Segmentation of Fluorescence Micrographs

Tim W. Nattkemper¹, Heiko Wersing¹
Walter Schubert^{2,3}, Helge Ritter¹

¹Neuroinformatics Group, University of Bielefeld, Germany,
email: {tnattkem,hwersing,helge}@techfak.uni-bielefeld.de

²Neuroimmunology and Molecular Pattern Recognition Group, University of Magdeburg

³MELTEC Ltd., University of Magdeburg, email:schubert@pc.mdlink.de

Abstract. A system for the automatic segmentation of fluorescence micrographs is presented. In a first step positions of fluorescent cells are detected by a fast learning neural network, which acquires the visual knowledge from a set of training cell-image patches selected by the user. Guided by the detected cell positions the system extracts in the second step the contours of the cells. For contour extraction a recurrent neural network model is used to approximate the cell shapes. Even though the micrographs are noisy and the fluorescent cells vary in shape and size, the system detects at minimum 95% of the cells.

1 Introduction

In the last decades experimental research in biomedicine was influenced by automation of sample preparation and digital microscopy imaging. Research groups in related fields are now enabled to produce large sets of digitized micrographs. Hence the problem of efficient evaluation of large datasets arises, for example in the case of high-throughput analysis of biopsies. In this work we present an architecture for automatic evaluation of fluorescence micrographs. The micrographs are grey value images, recorded by a CCD camera-equipped microscope. The images were generated with a standardized fluorescence microscopy technique, developed by the biomedical research group at the University of Magdeburg. The images show fluorescent lymphocyte cells in tonsil tissue. For the purpose of a final data analysis in each image the fluorescent cells have to be detected and the contour of each fluorescent cell has to be extracted. The contour information is needed to measure the grey value intensity distribution across the cell body which is an important cell feature to the biomedical researcher.

Evaluation of large numbers of micrographs by human experts is almost impossible because during the visual inspection of noisy intensity images the observer's concentration decreases rapidly, which makes the evaluation time consuming and leads to non-reproducible results.

In this paper we present a system for automatic evaluation of the fluorescence micrographs. An image is processed in two steps: In the first step the positions of fluorescent cells are detected by a pre-trained neural network, in the second step the detected cell

positions are used as “focus points” for guiding the system to the cells in the image. In the focused image patches a recurrent neural network is used to extract the cell contour. Segmentation algorithms in related computer vision applications are usually based on (i) flooding schemes in gradient mountains [Meyer and Beucher, 1990], (ii) wave propagation [Hanahara and Hiyane, 1990], (iii) boundary tracing [Galbraith et al., 1991] or (iv) backtracking search through combinations of line segments by calculating a saliency measure [Jacobs, 1996]. In our present study the considered objects are lymphocytes in tissue, so their shapes show considerable variation and are called *mainly convex*. This makes it very difficult to define one common contour model, which fits for all cells in the image. Furthermore, since the images are generated by immunofluorescence, heterogenous signals, reflecting different concentrations of cell surface proteins, cause local distortions in the cells’ contours.

2 The Fluorescence Micrograph Segmentation System

The architecture of the system is shown in figure 1. The system consists of two main modules. The first module performs the detection of fluorescent cells as focus points (see arrow (1) in fig. 1). It consists of a neural classifier which is trained to compute *evidence values* for each image point. The evidence values represent the probability that a point is occupied by a fluorescent cell. The positions of the fluorescent cells are computed by a simple post-processing of the evidence values.

The second module extracts at each focus point the cell contour (see arrow (2) in fig. 1) by a local figure-ground separation which is performed by a recurrent neural network for each cell, separately. The network is designed for making convex structures “pop-out” within a focused image region. The result of this separation is used to extract the contour line of the cell. The training of the cell detection and the two modules are explained in the following subsections.

2.1 Cell Detection with the Local Linear Map

The training and the application of the first module is explained only draftly (for details see [Nattkemper et al., 1999]). For detection of the fluorescent cells we use a neural network of local linear map-type (LLM) [Ritter, 1991]. To train the LLM a set of image patches containing cells as positive training examples is labeled by a biomedical expert using a computer mouse. The patch size is set to 15×15 pixels so that it covers the whole fluorescent cell body. A second set of negative examples is generated by choosing randomly from the same image a number of patch centers subject to the condition of having a distance of at least 5 pixels to each of the patches from the positive example set. For each patch a 6-dimensional feature vector \mathbf{x} is computed using 6 filter masks, which are eigenvectors obtained from a principal component analysis on the set of hand-selected (i. e. , positive) cell patches. The eigenvectors are also referred to as *eigencells* (see left column in fig. 1). They belong to the six largest eigenvalues. Thus, the image patch of $15 \times 15 = 225$ dimensions is projected to a 6-dimensional subspace which covers the most of the patch variance. This is an established technique in Computer Vision (see [Turk and Pentland, 1991]). Calculating the feature vectors for

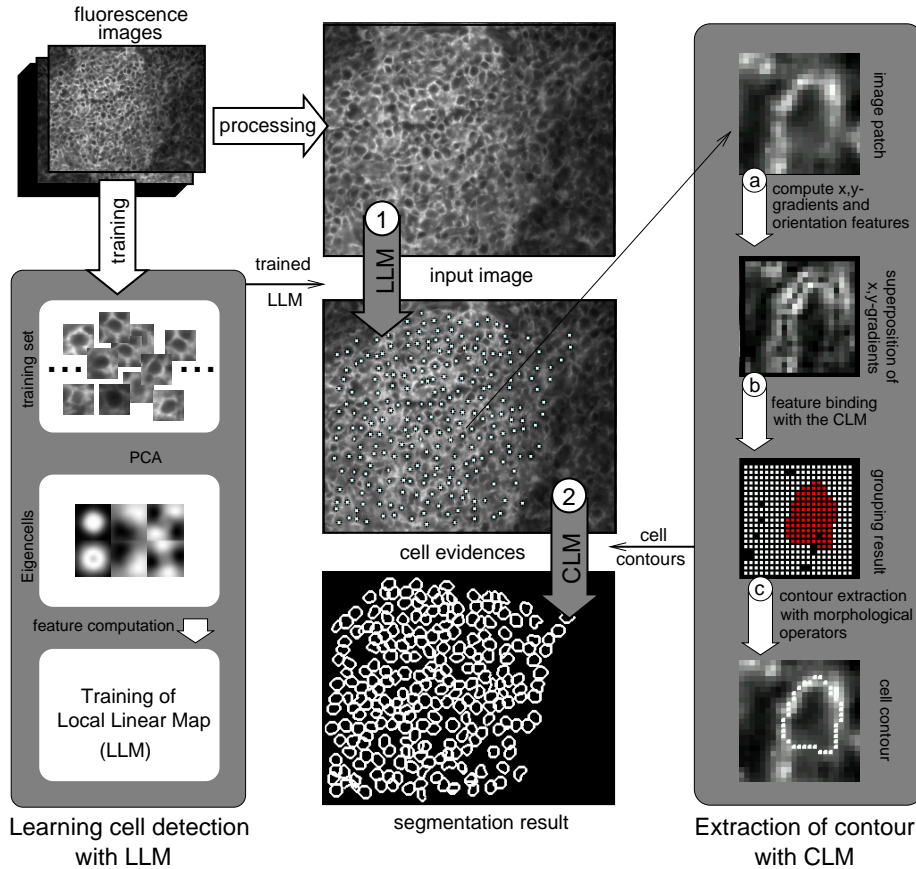


Fig. 1. An illustration of the segmentation system. See the text for details.

the positive and the negative input examples delivers the training set of (input, output)-pairs $T = \{(\mathbf{x}_i, \mathbf{y}_i)\}_i$, with $\mathbf{y}_i = 1$ if sample i is from the positive training set, $\mathbf{y}_i = 0$ otherwise.

The LLM combines unsupervised and supervised learning in contrast to the widely used multi-layer perceptron trained with back-propagation [Rumelhart et al., 1986]. The LLM learns a mapping $C : \mathbb{R}^{d_{in}} \mapsto \mathbb{R}^{d_{out}}$ by (i) a vector quantization of the input feature space based on T with a set of $l = 5$ reference vectors and (ii) an adaption of local linear mappings into the output space, which are attached to each reference vector. The trained LLM-classifier performs a mapping of image point features $\mathbf{x} \in \mathbb{R}^6$ to evidence values in $[0; 1]$ that represent the degree of belief that a fluorescent cell is positioned there. The evidence values written to the image coordinates of their corresponding image point form the so called *evidence map* of the input image. A thresholding procedure combined with a local maximum search in the evidence map finally delivers the positions of fluorescent cells.

2.2 Contour Extraction with the CLM

The second module performs the extraction of the cell contours. For each focus point its 20×20 -neighborhood is selected. This size is chosen to ensure that it includes the whole cell body. In this neighborhood the subregion which is occupied by the cell body is separated from its surrounding by figure-ground segmentation using the competitive layer model (CLM) [Ritter, 1990],[Wersing and Ritter, 1999] for feature binding, which can only be outlined in short. The CLM consists of two layers of topographically organized nodes. One layer is called the *ground* layer the other one the *figure* layer. Each node corresponds to one edge feature in the neighborhood and represents its tendency of grouping into one of the layers through its activity value. The grouping is achieved by high activities for cell-belonging nodes in the *figure* layer (grey dots in grouping result in fig. 1 and 2) and low activities of the same nodes in the *ground* layer (white dots in grouping result in fig.1 and 2), caused by competitive and cooperative interactions between the features. For features belonging to the surrounding of the cell body the nodes behave vice versa. The dynamical integration of noisy local edge orientations into a coherent cell body group achieves a very precise and noise resistant segmentation into cell body and background (fig. 1(b)). This way a segmentation of the neighborhood is achieved which is very robust due to the dynamical integration of noisy local curvature information into a coherent salient group, representing the fluorescent cell body.

To compute a one-pixel wide cell contour from the separated cell body region standard morphological closing- and erode-operators are applied [Sonka et al., 1993]. An illustration of the cell contour extraction is given in the right column of figure 1 and in fig. 2 below : For each point in the focussed neighborhood the orientation of the grey value gradient is computed as its edge feature (arrow (a) in fig. 1 and 2). After the grouping process (arrow (b) in fig. 1 and 2) the edge features are grouped in the ground layer (white dots) or in the figure layer (grey dots). Based on the separated cell body the contour is computed (arrow (c) in fig. 1 and 2).

3 Results

The segmentation system was applied to fluorescence images of lymphocytes in tonsil tissue. The 329×254 -sized images were recorded in a highly standardized procedure and show densely clustered fluorescent cells, which occlude each other partially. The results for two example images are shown in fig. 3. For measuring the correctness the

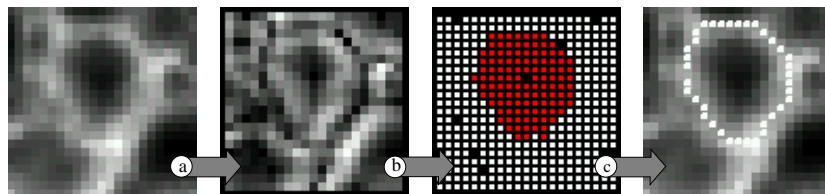


Fig. 2. Processing steps of the contour extraction. See text for details.

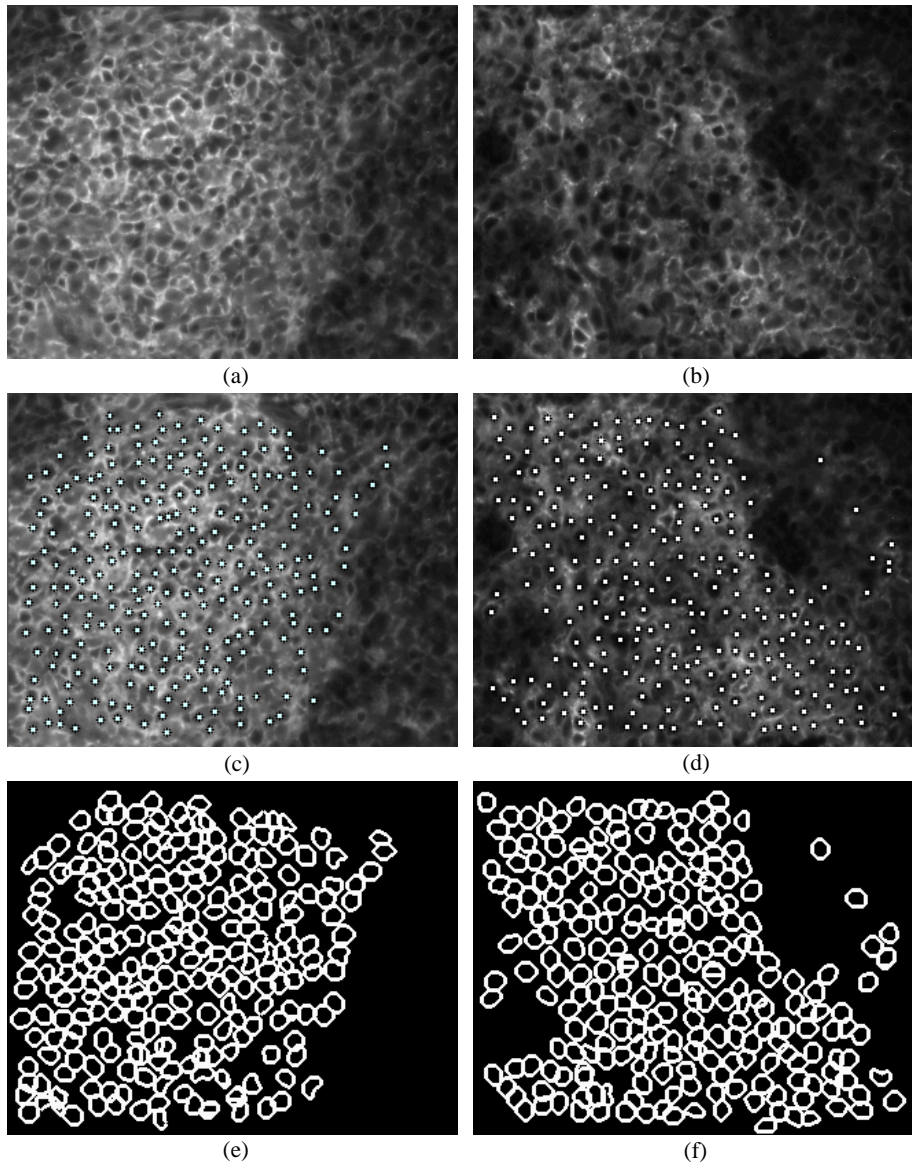


Fig. 3. The results for two fluorescence micrographs: Images (a) and (b) show two different fluorescence micrographs of lymphocytes in tonsil tissue. In the first step the positions of fluorescent cells are computed (see white dots in (c),(d)) for focussing. In the second step the cell contours are extracted for the fluorescent cells at the focus points. The contour extraction results are white plotted in images (e) and (f).

results were visually inspected by a highly experienced biomedical expert. According to the expert the system finds a minimum of 95% of the fluorescent cells (see fig. 3 (c),(d)) with a low rate of false positives of approximately 10%. The positions of the cells are

computed in less than 1 minute. The extraction of the cell contours for the detected cells with the CLM were sufficiently accurate, according to the expert. The CLM's segmentation performance remains constant under local distortions in the convexity of the contour in grey value intensity (see fig. 3 (e),(f)). The computation time for the contour detection of about 250 cells less than 2 minutes on a Pentium II 450 MHz double processor machine.

4 Conclusion

We presented a system for segmentation of fluorescence micrographs. The results were carefully inspected by a biomedical expert to measure accuracy and for comparison with human performance. It turned out that our approach works highly accurate and leads to reproducible results, in contrast to human employees. Thereby the system paves the way to automatic evaluation of this kind of microscope data, enabling high-throughput topological screening of lymphocytes in many types of tissue.

Acknowledgments: This work was supported by the DFG grants GK-231, Schu627/8-2, BMBF 07NBL04, BMBF 0311951, SFB 387 (TPB1).

References

- [Galbraith et al., 1991] Galbraith, W., Wagner, M., Chao, J., Abaza, M., Ernst, L., Nederlof, M., Hartsock, R., Taylor, D., and Waggoner, A. (1991). Imaging cytometry by multiparameter fluorescence. *Cytometry*, 12:579–596.
- [Hanahara and Hiyane, 1990] Hanahara, K. and Hiyane, M. (1990). A circle-detection algorithm simulating wave propagation. *Machine Vision and Applications*, 3:97–111.
- [Jacobs, 1996] Jacobs, D. W. (1996). Robust and efficient detection of salient convex groups. *IEEE Trans. on Pattern Analysis and Machine Intelligence*, 18(1):23–37.
- [Meyer and Beucher, 1990] Meyer, F. and Beucher, S. (1990). Morphological segmentation. *J. Visual Communications and Image Representation*, 1(1):21–46.
- [Nattkemper et al., 1999] Nattkemper, T. W., Ritter, H., and Schubert, W. (1999). Extracting patterns of lymphocyte fluorescence from digital microscope images. In *Intelligent Data Analysis in Medicine and Pharmacology 99 (IDAMAP), Workshop Notes*, pages 79–88.
- [Ritter, 1990] Ritter, H. (1990). A spatial approach to feature linking. In *Int. Neur. Netw. Conf. Proc. Paris*, volume 2, pages 898–901. Kluwer Publishers.
- [Ritter, 1991] Ritter, H. (1991). Learning with the self-organizing map. In Kohonen, T., editor, *Artificial Neural Networks 1*. Elsevier Science Publishers, B.V.
- [Rumelhart et al., 1986] Rumelhart, D., Hinton, G., and Williams, R. (1986). Learning internal representations by error propagation. *Parallel Distributed Processing: Explorations in the Microstructure of Cognition*, 1:Foundations:318–362.
- [Sonka et al., 1993] Sonka, M., Hlavac, V., and Boyle, R. (1993). *Image Processing, Analysis and Machine Vision*. Chapman & Hall.
- [Turk and Pentland, 1991] Turk, M. and Pentland, A. (1991). Eigenfaces for recognition. *Journal of Cognitive Neuroscience*, 3:71–86.
- [Wersing and Ritter, 1999] Wersing, H. and Ritter, H. (1999). Feature binding and relaxation labeling with the competitive layer model. In *Proc. Eur. Symp. on Art. Neur. Netw. ESANN*, pages 295–300.